

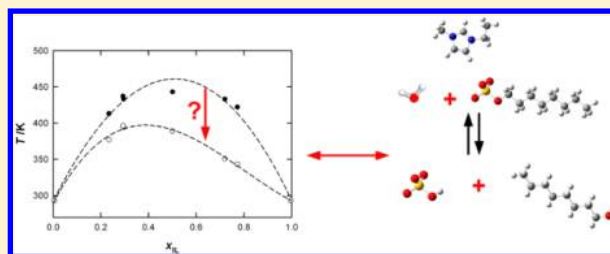
Are Alkyl Sulfate-Based Protic and Aprotic Ionic Liquids Stable with Water and Alcohols? A Thermodynamic Approach

Johan Jacquemin,* Peter Goodrich,* Wei Jiang, David W. Rooney, and Christopher Hardacre

The School of Chemistry and Chemical Engineering/QUILL Research Centre, Queen's University of Belfast, David Keir Building, Stranmillis Road, Belfast BT9 5AG, Northern Ireland, U.K.

Supporting Information

ABSTRACT: The knowledge of the chemical stability as a function of the temperature of ionic liquids (ILs) in the presence of other molecules such as water is crucial prior to developing any industrial application and process involving these novel materials. Fluid phase equilibria and density over a large range of temperature and composition can give basic information on IL purity and chemical stability. The IL scientific community requires accurate measurements accessed from reference data. In this work, the stability of different alkyl sulfate-based ILs in the presence of water and various alcohols (methanol, ethanol, 1-butanol, and 1-octanol) was investigated to understand their stability as a function of temperature up to 423.15 K over the hydrolysis and transesterification reactions, respectively. From this investigation, it was clear that methyl sulfate- and ethyl sulfate-based ILs are not stable in the presence of water, since hydrolysis of the methyl sulfate or ethyl sulfate anions to methanol or ethanol and hydrogenate anion is undoubtedly observed. Such observations could help to explain the differences observed for the physical properties published in the literature by various groups. Furthermore, it appears that a thermodynamic equilibrium process drives these hydrolysis reactions. In other words, these hydrolysis reactions are in fact reversible, providing the possibility to re-form the desired alkyl sulfate anions by a simple transesterification reaction between hydrogen sulfate-based ILs and the corresponding alcohol (methanol or ethanol). Additionally, butyl sulfate- and octyl sulfate-based ILs appear to follow this pattern but under more drastic conditions. In these systems, hydrolysis is observed in both cases after several months for temperatures up to 423 K in the presence of water. Therein, the partial miscibility of hydrogen sulfate-based ILs with long chain alcohols (1-butanol and 1-octanol) can help to explain the enhanced hydrolytic stability of the butyl sulfate- and octyl sulfate-based ILs compared with the methyl or ethyl sulfate systems. Additionally, rapid transesterification reactions are observed during liquid–liquid equilibrium studies as a function of temperature for binary systems of (hydrogen sulfate-based ionic liquids + 1-butanol) and of (hydrogen sulfate-based ionic liquids + 1-octanol). Finally, this atom-efficient catalyst-free transesterification reaction between hydrogen sulfate-based ILs and alcohol was then tested to provide a novel way to synthesize new ILs with various anion structures containing the alkyl sulfate group.



INTRODUCTION

Due to their very low volatility under ambient conditions, ionic liquids (ILs) are often classified as novel and green materials,^{1,2} even if this classification does not take into account other properties such as toxicity and chemical or thermal stability.³ The knowledge, over a large temperature range, of the density of pure ILs and their fluid phase equilibria in mixtures with other molecular compounds reflects the purity and the chemical stability of studied samples, and such information is crucial for novel materials like ILs. It is very well documented by ourselves^{4–6} and others^{7–11} that the presence of impurities like water and/or halogenated compounds dramatically changes the physical properties of ILs. In that sense, the identification of the impurities in the samples is of particular importance. Furthermore, it was recently reported in the literature that some ILs, for example, based on hexafluorophosphate ([PF₆]⁻) and tetrafluoroborate ([BF₄]⁻) are not water-stable since they hydrolyze easily in the presence of water.^{12,13} In this regard, more stable hydrophilic fluorine-based anions such as bis-

(trifluoromethylsulfonyl)imide ([NTf₂]⁻) and the tris-(perfluoroalkyl)trifluorophosphate ([FAP]⁻) have been developed. The stability of these anions is well-established and these salts have found many applications in the fields of catalysis; however, one major drawback is their expense.¹⁴ This has, in turn, led to the development of cheaper halide-free ILs, such as those based on the alkyl sulfate, alkyl phosphate, and alkyl carbonate anions. Of these, the alkyl sulfate ILs, of which the ethyl analogue is industrially available, have received particular attention.¹⁵ Despite the potential applications provided, these ILs are also known to be hydrolytically unstable. Wasserscheid et al. reported rapid hydrolysis of 1-ethyl-3-methylimidazolium ethyl sulfate, [C₁C₂Im][EtSO₄], by contaminating it artificially with a large excess of water at 353 K.¹⁶ Ficke et al. have also demonstrated that this IL decomposes to ethanol and 1-ethyl-3-

Received: December 12, 2012

Revised: January 10, 2013

Published: January 15, 2013

methylimidazolium hydrogenosulfate, $[C_1C_2Im][HSO_4]$, over extended time periods.¹⁷ This information is of great importance in this field and must be taken into account in determining reference data. Therein, our group recently published a critical overview of our previously reported density studies,¹⁸ with more than 1800 data available from the literature over temperature and pressure ranges from 293 to 415 K and 0.1 to 40 MPa, respectively.¹⁹ This investigation has clearly indicated again that ethyl sulfate-based ILs are not water-stable and time-stable compounds, since they hydrolyze at room temperature even in presence of any trace amounts of moisture coming from the atmosphere. Nevertheless, to date, limited information about the reaction process between alkyl sulfate-based ILs with water is available in the literature. It is well-known that reversible hydrolysis reactions are often coupled with transesterifications reactions. In that sense, Himmeler et al.²⁰ have reported a new synthetic method to produce alkyl sulfate ionic liquids based on a transesterification reaction between methyl sulfate or ethyl sulfate ionic liquids and a long-chain alcohol (1-butanol, 1-hexanol, 1-octanol, 2-methoxyethanol, 2-ethoxyethanol, 2-butoxyethanol, diethyleneglycol monoethyl ether and diethyleneglycol monomethyl ether) in the presence of a Brønsted acid catalyst (0.4 mol % methanesulfonic acid). More recently, hydrolysis of methyl sulfate and ethyl sulfate was reported by Ferguson et al.,²¹ from which it appears that a complete hydrolysis reaction of methyl sulfate (ethyl sulfate) to the hydrogen sulfate anion is obtained through the addition of 2 mol·L⁻¹ of the methyl sulfate (ethyl sulfate) ILs in an aqueous solution containing 40 mol % of sulfuric acid solution stirred at 373 K for 5 h. Nevertheless, to date, all the reported hydrolysis²¹ and transesterification²⁰ reactions have been realized in the presence of a Brønsted acid catalyst, which cannot explain the low hydrolytic and transesterification stabilities of alkyl sulfate-based ILs in the presence of only water or alcohols, respectively.

As density data is often used as a probe for the purity of the investigated materials, the density of seven pure ILs {1-ethyl-3-methylimidazolium hydrogen sulfate, $[C_1C_2Im][HSO_4]$; 1-ethyl-3-methylimidazolium methyl sulfate, $[C_1C_2Im][MeSO_4]$; 1-ethyl-3-methylimidazolium ethyl sulfate, $[C_1C_2Im][EtSO_4]$; 1-ethyl-3-methylimidazolium octyl sulfate, $[C_1C_2Im][OcSO_4]$; 1-butyl-3-methylimidazolium methyl sulfate, $[C_1C_4Im][MeSO_4]$; tributylmethylammonium methyl sulfate, $[N_{1444}][MeSO_4]$; and 1-butyl-1-methylpyrrolidinium methyl sulfate, $[C_1C_4Pyrro][MeSO_4]$ } was measured as a function of temperature from (293 to 363) K at atmospheric pressure to first confirm previous data published by our group for $[C_1C_2Im][EtSO_4]$ ^{4,5,18,22} and to evaluate these data with those already published by others.^{23–32} Second, an attempt was performed to estimate from the density data the effective molar volume of each unknown ion by using the methodology already published by our group,⁵ i.e., to extend as the function of temperature the observed differences highlighted by Costa et al.²⁴ in the effective molar volume of the hydrogen sulfate anion in comparison with those calculated in the case of aprotic alkyl sulfate ILs. Third, the mutual solubility of $[C_1C_2Im][HSO_4]$ with linear alcohols was investigated by measuring the clear and cloud point temperatures using a standard nephelometric method, and the chemical stability of each studied mixture was then checked through NMR measurements. Hydrolysis and transesterification reactions between the studied ILs with water and with alcohols, respectively, were then investigated by using three types of reactor—open and sealed with or without headspace—in order to study the chemical and thermal stabilities of each binary

mixture with the temperature. Such stabilities were then verified by using NMR spectroscopy. Finally, the hydrolysis/trans-esterification reactions between alkyl sulfate anions and water/alcohol were then investigated by using G3 Gaussian calculations of each species involved as a function of temperature. These simulations were then compared with the experimental results.

MATERIALS AND METHODS

Materials. Chemicals. The reagents used for the synthesis of ILs were supplied by Aldrich [tributylamine (99%), 1-butylpyrrolidine (99%), 1-butylimidazole (99%), 1-methylimidazole (99%), dimethyl sulfate (99%), diethyl sulfate (99%), benzyl alcohol (99%), butylamine (99%), *N,N*-diisopropylaminoethanol (99%) and 2,2,3,3,4,4,4-heptafluoro-1-butanol (98%)]. Toluene (HPLC grade) and ethyl acetate (HPLC grade) were supplied by Riedel-de-Haen. All chemicals and reagents were used without any further purification. 1-Ethyl-3-methylimidazolium hydrogen sulfate and the corresponding octyl sulfate were kindly supplied by BASF and Merck, respectively, and were used after drying under high vacuum (1 Pa) at 333 K overnight.

General Procedure for the Synthesis of Alkyl Sulfate-Based ILs. All ILs were prepared according to the following procedure: dialkyl sulfate (0.2 mol) dissolved in anhydrous toluene (50 mL) was added slowly dropwise to a precooled solution of amine (0.2 mol) in anhydrous toluene (150 mL). The mixture was continually cooled in an ice-bath under nitrogen with care being taken to maintain the reaction temperature below 298 K. After complete addition of the dialkyl sulfate, the reaction mixture was then stirred at room temperature for 4 h. The upper organic phase of the resulting mixture was decanted, and the lower IL phase was washed with ethyl acetate (3 × 20 mL). After washing, the remaining ethyl acetate and any residual water was removed by heating under reduced pressure. All ILs were obtained with more than 98% of purity. Their structures were confirmed by comparison of ¹H NMR available in the literature (see Supporting Information, Figures S1–S6).^{23–26}

1-Ethyl-3-methylimidazolium Methyl Sulfate, $[C_1C_2Im][MeSO_4]$. ¹H NMR (300 MHz, DMSO capillary, ppm): 9.38 (s, 1H, H-2), 7.57 (s, 2H, H-4 and H-5), 4.31 (q, *J* = 7.2 Hz, 2H, NCH₂CH₃), 4.01 (s, 3H, NCH₃), 3.70 (s, 3H, OCH₃), 1.55 (t, *J* = 7.2 Hz, 3H, NCH₂CH₃).

1-Butyl-3-methylimidazolium Methyl Sulfate, $[C_1C_4Im][MeSO_4]$. ¹H NMR (300 MHz, DMSO capillary, ppm): 9.06 (s, 1H, H-2), 7.77 (s, 1H, H-4), 7.68 (s, 1H, H-5), 4.14 (q, *J* = 7.4 Hz, 2H, NCH₂CH₂), 3.87 (s, 3H, NCH₃), 3.42 (s, 3H, OCH₃), 1.67 (m, 2H, NCH₂CH₂), 1.09 (m, 2H, N(CH₂)₂CH₂), 0.64 (t, *J* = 7.1 Hz, 3H, N(CH₂)₃CH₃).

1-Butyl-1-methylpyrrolidinium Methyl Sulfate, $[C_1C_4Pyrro][MeSO_4]$. ¹H NMR (300 MHz, DMSO capillary, ppm, δ): 3.66 (s, 3H, OCH₃), 3.39 (m, 4H, NCH₂), 3.23 (m, 2H, NCH₂), 2.93 (s, 3H, NCH₃), 2.11 (m, 4H, NCH₂CH₂), 1.66 (m, 2H, NCH₂CH₂), 1.29 (sextuplet, *J* = 7.4 Hz, 2H, N(CH₂)₂CH₂), 0.85 (t, 3H, *J* = 7.4 Hz, N(CH₂)₃CH₃).

Tributylmethylammonium Methyl Sulfate, $[N_{1444}][MeSO_4]$. ¹H NMR (300 MHz, DMSO, ppm, δ): 3.39 (s, 3H, OCH₃), 3.19 (m, 6H, NCH₂), 2.96 (s, 3H, NCH₃), 1.59 (m, 6H, NCH₂CH₂), 1.32 (q, *J* = 7.5 Hz, 6H, N(CH₂)₂CH₂), 0.95 (t, *J* = 7.3 Hz, 9H, N(CH₂)₃CH₃).

1-Ethyl-3-methylimidazolium Ethyl Sulfate, $[C_1C_2Im][EtSO_4]$. ¹H NMR (300 MHz, DMSO capillary, ppm): 9.39 (s, 1H, H-2), 7.73 (s, 2H, H-4 and H-5), 4.34 (q, *J* = 7.4 Hz, 2H, NCH₂CH₃), 4.12 (q, *J* = 7.0 Hz, 2H, OCH₂CH₃), 4.06 (s, 3H,

Table 1. Structure, Source, Molecular Purity, Molar Mass (M_{IL}) of Each Selected Dried ILs Sample

<i>Ionic Liquid</i>	<i>Structure</i>	<i>Source</i>	<i>Purity / mol%</i>	$M_{IL} / \text{g}\cdot\text{mol}^{-1}$
$[\text{C}_1\text{C}_2\text{Im}][\text{HSO}_4]$		BASF	> 95.0 ^a	208.24
$[\text{C}_1\text{C}_2\text{Im}][\text{OcsO}_4]$		Merck	> 98.0 ^a	320.45
$[\text{C}_1\text{C}_2\text{Im}][\text{MeSO}_4]$				222.26
$[\text{C}_1\text{C}_2\text{Im}][\text{EtSO}_4]$				236.29
$[\text{C}_1\text{C}_4\text{Im}][\text{MeSO}_4]$		QUILL	> 98.0 ^b	250.31
$[\text{C}_1\text{C}_4\text{Pyrro}][\text{MeSO}_4]$				253.36
$[\text{N}_{1444}][\text{MeSO}_4]$				311.48

^aPurity estimated by the supplier. ^bPurity estimated by NMR analysis (see Supporting Information)

NCH_3), 1.79 (t, $J = 7.33$ Hz, 3H, NCH_2CH_3), 1.17 (t, $J = 6.9$ Hz, 3H, OCH_2CH_3).

After treating the ILs for 15 h at room temperature under vacuum (lower than 1 Pa), the sample was considered as dried and was then stored under nitrogen atmosphere to avoid water contamination from atmosphere. Each IL was analyzed for water content using Coulometric Karl Fischer titration (Mettler Toledo DL31) prior to all measurements. These measurements revealed very low levels of water, always lower than 250 ppm, i.e., lower than 0.025 wt %, except in the case of the $[\text{C}_1\text{C}_2\text{Im}][\text{HSO}_4]$, where the water content in this IL was found to be close to 2000 ppm, i.e. ~ 0.2 wt %). The structure, source, and molecular purity of each IL studied are reported in Table 1.

Experimental Methods. Density Measurements. The experimental apparatus used to measure the densities was a U-shape vibrating-tube densitometer (Anton Parr 4500) operating in a static mode and was calibrated as previously described by our group.⁵ The effect of viscosity on the density data as a function of temperature was then taken into account by using viscosity data already available in the literature for each pure IL.^{23–25}

Liquid–Liquid Equilibria. The (liquid + liquid) miscibility gap was measured using a standard nephelometric method.^{22,33} In this technique, the miscibility is determined by finding visually the clear and cloud points temperatures at which a phase change occurs in a binary mixture of known composition (gravimetrically determined). The relative uncertainty on the mass fraction is estimated to be less than 2×10^{-4} . All binary mixtures were placed in a thermostated equilibrium cell. The clear point temperature was then obtained by increasing the temperature at which the mixture becomes entirely homogeneous. The cloud point temperatures were then visually determined by decreasing the temperature until the first droplet of the second phase appeared. Different heating and cooling cycles have been measured to quantify the difference in the read-outs during each cycle, in order to investigate the stability of each mixture

with the temperature. The temperature was measured using a 100 Ω platinum resistance thermometer (precision of ± 0.1 K and accuracy of ± 0.5 K). On the basis of a statistical analysis of the present data, the uncertainty of the cloud point is estimated as to be close to ± 0.5 K.

Monitoring of Hydrolysis and Transesterification Reactions. Chemical and thermal stabilities of the (IL + water) and (IL + *n*-alcohol) binary mixtures were investigated as a function of the temperature up to 423 K by using three different types of reactors. Open and sealed with and without headspace reactor types were selected in order to investigate the effect of the presence or absence of the vapor phase on their stabilities. The stabilities were analyzed by studying each sample without any purification by ^1H NMR and ^{13}C NMR in the presence of a sealed capillary tube containing deuterated D_2O or DMSO using a Bruker AVANCE 300 MHz NMR. The limits of detection for NMR when using a deuterated solvent capillary tube are approximately $\pm 2\%$.³⁴

RESULTS AND DISCUSSION

Volumetric Properties of Pure ILs. Density measurements of the pure ILs were carried out at temperatures ranging from 293.15 to 363.15 K at 0.1 MPa. The melting point of the pure $[\text{N}_{1444}][\text{MeSO}_4]$ has been reported as close to 335.15 K,³⁵ but we observed that this IL remains as a subcooled liquid for several hours at room temperature (≈ 293 K). This behavior has been already reported in the case of other alkyl sulfate-based ILs,^{16,36,37} providing then the possibility to measure their thermodynamic properties in this subcooled state. Herein, the liquid density of $[\text{N}_{1444}][\text{MeSO}_4]$ has been measured from 293 K, i.e., above its melting point temperature. The experimental data for all the pure ILs are reported in Table 2 and shown in Figure 1.

For the pure ILs, the density values typically vary from 1.05 to $1.37 \text{ g}\cdot\text{cm}^{-3}$ at 293 K and from 1.01 to $1.33 \text{ g}\cdot\text{cm}^{-3}$ at 363 K. As

Table 2. Experimental Densities (ρ) and Molar Volumes (V_m) of Dried ILs as a Function of Temperature at Atmospheric Pressure

T/K	[C ₁ C ₂ Im][HSO ₄]		[C ₁ C ₂ Im][MeSO ₄]		[C ₁ C ₂ Im][EtSO ₄]	
	$\rho/\text{g}\cdot\text{cm}^{-3}$	$V_m/\text{cm}^3\cdot\text{mol}^{-1}$	$\rho/\text{g}\cdot\text{cm}^{-3}$	$V_m/\text{cm}^3\cdot\text{mol}^{-1}$	$\rho/\text{g}\cdot\text{cm}^{-3}$	$V_m/\text{cm}^3\cdot\text{mol}^{-1}$
293.15	1.3689	152.12	1.2895	172.36	1.2411	190.39
298.15	1.3659	152.46	1.2861	172.82	1.2376	190.92
303.15	1.3628	152.80	1.2826	173.29	1.2341	191.47
313.15	1.3568	153.48	1.2758	174.21	1.2274	192.51
323.15	1.3508	154.16	1.2691	175.13	1.2207	193.57
333.15	1.3447	154.86	1.2624	176.06	1.2140	194.64
343.15	1.3387	155.55	1.2558	176.99	1.2074	195.70
353.15	1.3326	156.27	1.2493	177.91	1.2008	196.78
363.15	1.3266	156.97	1.2429	178.82	1.1942	197.86
T/K	[C ₁ C ₂ Im][OCSO ₄]		[C ₁ C ₄ Im][MeSO ₄]			
	$\rho/\text{g}\cdot\text{cm}^{-3}$	$V_m/\text{cm}^3\cdot\text{mol}^{-1}$	$\rho/\text{g}\cdot\text{cm}^{-3}$	$V_m/\text{cm}^3\cdot\text{mol}^{-1}$		
293.15	1.0987	291.66	1.2144	206.12		
298.15	1.0953	292.57	1.2110	206.70		
303.15	1.0920	293.45	1.2077	207.27		
313.15	1.0854	295.24	1.2010	208.42		
323.15	1.0789	297.02	1.1944	209.57		
333.15	1.0724	298.82	1.1879	210.72		
343.15	1.0659	300.64	1.1814	211.88		
353.15	1.0595	302.45	1.1749	213.05		
363.15	1.0532	304.26	1.1685	214.22		
T/K	[C ₁ C ₄ PyrrO][MeSO ₄]		[N ₁₄₄₄][MeSO ₄]			
	$\rho/\text{g}\cdot\text{cm}^{-3}$	$V_m/\text{cm}^3\cdot\text{mol}^{-1}$	$\rho/\text{g}\cdot\text{cm}^{-3}$	$V_m/\text{cm}^3\cdot\text{mol}^{-1}$		
293.15	1.1699	216.56	1.0591	294.10		
298.15	1.1670	217.10	1.0562	294.91		
303.15	1.1638	217.70	1.0531	295.77		
313.15	1.1575	218.88	1.0470	297.50		
323.15	1.1517	219.99	1.0409	299.24		
333.15	1.1455	221.18	1.0347	301.03		
343.15	1.1395	222.34	1.0286	302.82		
353.15	1.1337	223.48	1.0225	304.63		
363.15	1.1279	224.63	1.0165	306.42		

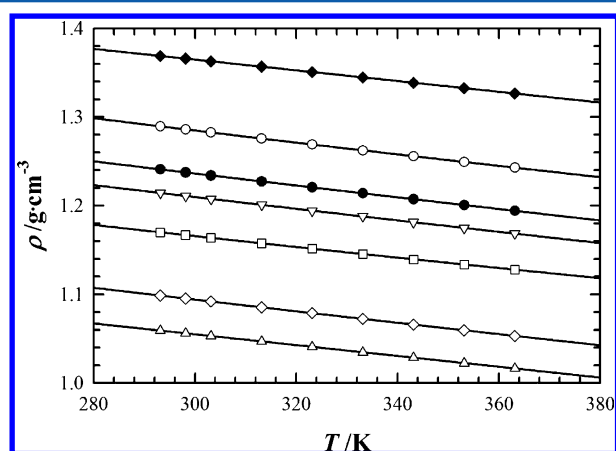


Figure 1. Experimental densities of dried (Δ) [N₁₄₄₄][MeSO₄], (\square) [C₁C₄PyrrO][MeSO₄], (∇) [C₁C₄Im][MeSO₄], (\blacklozenge) [C₁C₂Im]-[HSO₄], (\circ) [C₁C₂Im][MeSO₄], (\bullet) [C₁C₂Im][EtSO₄], and (\diamond) [C₁C₂Im][OCSO₄] as a function of the temperature at 0.1 MPa. The lines correspond to the fit of the data by eq 1 reported in Table 3.

expected, the density is found to decrease with increasing the alkyl chain length on both the alkyl sulfate anion and on the imidazolium cation. Furthermore, Figure 1 also shows that the density of the ILs based on the [MeSO₄]⁻ anion increased in the following order: [N₁₄₄₄]⁺ < [C₁C₄PyrrO]⁺ < [C₁C₄Im]⁺ <

[C₁C₂Im]⁺. These trends are in good agreement with the variation in density with the IL structure previously reported in the literature.^{38,39} The variation of the density with temperature for the ILs studied is illustrated in Figure 1. The polynomial equation used to fit this variation with temperature was of the form

$$\rho_{\text{IL}}(T) = a + b(T) + c(T)^2 \quad (1)$$

with the parameters a , b , and c , and standard deviations σ_ρ are given in Table 3.

Molar volumes, V_m , of dried ionic liquids were then calculated via eq 2

$$V_{m,\text{IL}} = \frac{M_{\text{IL}}}{\rho_{\text{IL}}} \quad (2)$$

where M_{IL} and ρ_{IL} are the molar mass and the density of the studied ionic liquid, respectively.

The calculated molar volumes are reported in Table 2 as function of temperature up to 363.15 K. As expected, the IL molar volumes increase with the temperature and the alkyl chain length on the cation. This result is in good agreement with results already available in the literature for different IL structures.^{38,39} Furthermore, from the work of Rebelo and co-workers,⁴⁰ who reported that the excess molar volumes of IL mixtures can be considered as ideal (e.g., $V^E \approx 0 \text{ cm}^3\cdot\text{mol}^{-1}$), our group

Table 3. Correlation Parameters a , b , and c and Standard Deviation, σ_ρ , of Eq 1 for the Density of Dried ILs as a Function of Temperature Determined from Measurements between 293.15 and 363.15 K

ionic liquid	$a/\text{g}\cdot\text{cm}^{-3}$	$10^4 \times b/\text{g}\cdot\text{cm}^{-3}\cdot\text{K}^{-1}$	$10^7 \times c/\text{g}\cdot\text{cm}^{-3}\cdot\text{K}^{-2}$	$10^4 \times \sigma_\rho/\text{g}\cdot\text{cm}^{-3}$
[C ₁ C ₂ Im][HSO ₄]	1.54609	-6.045	0.00280	0.34
[C ₁ C ₂ Im][MeSO ₄]	1.52627	-9.218	3.894	0.27
[C ₁ C ₂ Im][EtSO ₄]	1.46283	-8.278	2.429	0.56
[C ₁ C ₂ Im][OcSO ₄]	1.31622	-8.167	2.543	0.33
[C ₁ C ₄ Im][MeSO ₄]	1.43255	-8.278	2.448	0.28
[C ₁ C ₄ Pyrrro][MeSO ₄]	1.38160	-8.188	3.308	1.1
[N ₁₄₄₄][MeSO ₄]	1.23977	-6.203	0.1457	0.66

^a $\sigma_\rho = (\sum(\rho_i^{\text{exp}} - \rho_i^{\text{calc}})^2/n - \nu)^{0.5}$, where n is the number of experimental points and ν is the number of adjustable parameters.

Table 4. Parameters Associated with Eq 4 Used To Predict the Molar Volume of Selected ILs as the Function of Temperature and 0.1 MPa from the Effective Molar Volume of Ions Available in the Literature,^{5,41} along with the Relative Absolute Average Deviations (RAAD; see eq 5) between the Calculated Molar Volumes and Those Presented during This Work (Table 2)

ion	$M/\text{g}\cdot\text{mol}^{-1}$	Effective Molar Volumes/ $\text{cm}^3\cdot\text{mol}^{-1}$		
		$C_0/\text{cm}^3\cdot\text{mol}^{-1}$	$10^2 \times C_1/\text{cm}^3\cdot\text{mol}^{-1}\cdot\text{K}^{-1}$	$10^5 \times C_2/\text{cm}^3\cdot\text{mol}^{-1}\cdot\text{K}^{-2}$
[C ₁ C ₂ Im] ⁺ ⁵	111.17	100.02	+6.955	+2.996
[C ₁ C ₄ Im] ⁺ ⁵	139.22	134.26	+8.890	+4.304
[C ₁ C ₄ Pyrrro] ⁺ ⁵	142.26	145.03	+10.00	-6.600
[N ₁₄₄₄] ⁺ ⁵	200.38	222.13	+1.428	+340.9
[N ₁₄₄₄] ⁺ ^a	200.38	222.53	+14.38	+26.73
[HSO ₄] ⁻ ^a	97.07	52.442	-0.211	+0.110
[MeSO ₄] ⁻ ⁵	111.10	72.397	+2.692	-16.82
[EtSO ₄] ⁻ ⁵	125.12	90.681	+3.158	-6.914
[OcSO ₄] ⁻ ⁵	209.28	191.40	+13.66	-31.62

Comparison between Calculated and Experimental Molar Volumes from 293 to 363 K at 0.1 MPa

ionic liquid	100 × RAAD	ionic liquid	100 × RAAD
[C ₁ C ₂ Im][HSO ₄] ^b	0.002	[C ₁ C ₄ Im][MeSO ₄] ^c	0.083
[C ₁ C ₂ Im][MeSO ₄] ^c	0.271	[C ₁ C ₄ Pyrrro][MeSO ₄] ^c	0.141
[C ₁ C ₂ Im][EtSO ₄] ^c	0.212	[N ₁₄₄₄][MeSO ₄] ^c	0.483
[C ₁ C ₂ Im][OcSO ₄] ^c	0.267	[N ₁₄₄₄][MeSO ₄] ^b	0.005

^aCalculated during this work. ^bCalculated using new parameters presenting into this work (correlation). ^cCalculated using original parameters⁵ (prediction). Bold text is used to highlight large deviation between experimental molar volumes and those calculated using original parameters.⁵

formulated a group contribution model (GCM) that was able to predict, within an accuracy close to 0.5%, the volumetric properties of pure ILs as a function of the temperature⁵ and the pressure⁴¹ based on the following equations

$$V_m(T^*, p) = V_c^*(T^*, p) + V_a^*(T^*, p) \quad (3)$$

$$V_{\text{ion}}^*(T^*, p) = \sum_{i=0}^2 C_i(T^*, p)^i \quad (4)$$

where V_c^* and V_a^* are the cation and anion effective molar volumes, respectively, at the discrete temperature $T^* = T - 298.15$ K, and C_i is the effective molar volume group contribution parameters of each ion described by our group previously as a function of the discrete temperature, T^* at 0.1 MPa.^{5,41}

In our original paper,⁵ except for the case of the [HSO₄]⁻ anion, the effective molar volumes of all ions involved during this work were already defined at 0.1 MPa as a function of temperature. Herein, in order to test the accuracy of our model, the volumetric properties of each of the IL studies were predicted. These comparisons are presented in Table 4 together with the percent relative absolute average deviation (100 × RAAD) between density values reported, herein, and those calculated by our GCM,⁵ as a function of temperature up to 363.15 K.

$$100 \times \text{RAAD} = \frac{100}{N} \sum \left| \frac{\rho_{\text{exp}} - \rho_{\text{GCM}}}{\rho_{\text{GCM}}} \right| \quad (5)$$

with N being the total number of data used, ρ_{GCM} the density values calculated by our GCM,⁵ and ρ_{exp} the corresponding value obtained from our experimental work. The RAAD can be regarded as a measure of the accuracy of our GCM.

Furthermore, by using the same methodology as reported previously,⁵ new parameters that are able to determine the effective molar volume of the [HSO₄]⁻ anion were then calculated and also are reported in Table 4. For each of the studied ILs, the accuracy of our GCM is better than 0.3%, except in the case of [N₁₄₄₄][MeSO₄], where a deviation close to 0.5% is observed. The effective molar volume of the [N₁₄₄₄]⁺ has been calculated previously⁵ for a temperature range from 297 to 333 K using a density data set published by Anthony et al.⁴² for the IL [N₁₄₄₄][NTf₂]. Herein, the effective molar volume of [N₁₄₄₄]⁺ from 293 to 363 K was first recalculated by using the density data set in the case of [N₁₄₄₄][MeSO₄] reported in Table 2 with eqs 3 and 4. New effective molar volume fitting parameters of [N₁₄₄₄]⁺ are reported into Table 4 as a function of temperature up to 363 K and 0.1 MPa. Using this new set of parameters, a deviation up to 0.3% is then obtained by comparing experimental⁴² and calculated (using our GCM⁵) molar volumes for [N₁₄₄₄][NTf₂]

from 297 to 333 K at 0.1 MPa. Such deviations can be used to identify the accuracy of these fitting parameters.

As the density of all the selected ILs, except in the case of $[N_{1444}][MeSO_4]$, was already described by other groups in the literature, it was then possible to compare our reported experimental data as a function of temperature.^{23–32} Furthermore, it was then also possible to re-evaluate the accuracy of our previously published data in the case of $[C_1C_2Im][EtSO_4]$.^{4,5,18,22} These comparisons are presented in Table 5

Table 5. Relative Absolute Average Deviations RAAD (see eq 6) between the Densities Presented in This Work and Those of the Literature^{4,5,18,22–32}

ionic liquid	Nb data	T/K ^a	100 × RAAD	ref
$[C_1C_2Im][HSO_4]$	71	293–363	0.008	24
	6	293–343	0.025	31
$[C_1C_2Im][MeSO_4]$	71	293–363	0.003	24
	6	293–343	0.141	31
	4	298–328	3.54	32
$[C_1C_2Im][EtSO_4]$	7	293–352	0.266	4
	8	293–363	0.119	5
	7	293–352	0.265	18
	11	293–343	0.253	22
	71	293–363	0.021	30
	11	293–343	0.008	26
	^b	293–333	0.067	29
$[C_1C_2Im][OcsO_4]$	71	293–363	0.023	24
	^b	293–333	0.061	29
$[C_1C_4Im][MeSO_4]$	11	293–343	0.082	23
	8	293–308	0.089	27
	9	298–308	0.251	28
$[C_1C_4Pyrro][MeSO_4]$	10	298–343	0.014	25
$[N_{1444}][MeSO_4]$	–	–	–	–

^aEach reported temperature range corresponds to the T interval where each comparison was realized. ^bCalculated from fitting parameters for the linear temperature dependence of density from 293.15 to 333.15 K.²⁹ Bold text is used to highlight RAAD values higher than the expected uncertainty on density data.

together with the percent RAAD between density values reported herein and those available in the literature,^{4,5,18,22–32} for temperature ranging from 293 to 363 K at atmospheric pressure. In each case, the reported percent RAAD was calculated from the prior evaluation of each individual relative deviation (RD) reported in this temperature range between data from the literature with those presented herein according to the following equation

$$100 \times \text{RAAD} = \frac{100}{N} \sum \left| \frac{\rho_{\text{lit.}} - \rho_{\text{exp}}}{\rho_{\text{exp}}} \right| = \frac{100}{N} \sum |\text{RD}| \quad (6)$$

where N is the total number of data used, $\rho_{\text{lit.}}$ the density values from the literature, and ρ_{exp} the corresponding value obtained from our experimental work. The RAAD can be regarded as a measure of the accuracy of our experimental data and can be used as a probe of the purity of each IL.

According to the Table 5, density data sets of $[C_1C_2Im][HSO_4]$, $[C_1C_2Im][MeSO_4]$, $[C_1C_2Im][OcsO_4]$ published by Costa et al.²⁴ as well as those published in the case of $[C_1C_4Pyrro][MeSO_4]$ by Gonzalez et al.²⁵ are in excellent agreement with ours (RAAD close to 0.01% in each case), with

deviations within the experimental uncertainty. Similarly, the density data set published by Ficke et al.³¹ in the case of $[C_1C_2Im][HSO_4]$ is in excellent agreement with our (RAAD close to 0.03%). In the case of $[C_1C_2Im][MeSO_4]$, two other density data sets were compared with our data.^{31,32} For this IL, deviations up to 0.14% and 3.54% are observed as a function of temperature by comparing our density data set with those provided by Ficke et al.³¹ and by Shekaari et al.³² In each case, published density data are higher than ours. Even if an accuracy of 0.14% can be explained by taking into account each experimental uncertainty, in the case of the density of the $[C_1C_2Im][MeSO_4]$ published by Shekaari et al.³² an extremely high deviation, up to 3.54%, is observed with our data set. This observation is consistent with that made by Costa et al.²⁴ In the case of the $[C_1C_2Im][OcsO_4]$, two density data sets are available,^{24,29} and in each case, excellent agreement with our data is observed. The density of $[C_1C_4Im][MeSO_4]$ as a function of temperature is also available in the literature; the density reported herein is in good agreement with data published by Pereiro et al.²³ (RAAD \approx 0.08%) and by Krumelan et al.²⁷ (RAAD \approx 0.09%) for temperatures up to 343 K, as well as density data published at 298.15 K by Domańska et al.⁴³ within a deviation up to 0.1%. Nevertheless, in the case of $[C_1C_4Im][MeSO_4]$, the density data presented herein are systematically higher (RAAD \approx 0.25%) than those published by Navia et al.²⁸ Finally, in the case of $[C_1C_2Im][EtSO_4]$, excellent agreement is observed with the density data set provided by Gomez et al.²⁶ (RAAD \approx 0.01%), Russina et al.²⁹ (RAAD \approx 0.07%), Jacquemin et al.⁵ (RAAD \approx 0.12%), and de Castro et al.³⁰ (RAAD \approx 0.02%) as a function of temperature up to 363 K. The density data sets published by our group in different publications^{4,18,22} are higher than data presented herein. As already mentioned by our group,¹⁹ this density difference can be explained by a hydrolysis reaction that occurs over time between the ethyl sulfate anion and water. Therefore, we recommend not to use density data sets of $[C_1C_2Im][EtSO_4]$ published by our group in refs 4, 18, and 22 but to reference data reported herein or in refs 5, 19, 26, 29, and 30. Similarly, the large deviation observed between the density data set presented herein with that published by Shekaari et al.³² in the case of $[C_1C_2Im][MeSO_4]$ can be also explained by a hydrolysis reaction between the methyl sulfate anion and water. Nevertheless, to date very little data on such a reaction for IL media are available in the literature; for this reason, our group has then decided to investigate this problem.

Thermal Hydrolytic Stability of Alkyl Sulfate-Based ILs.

As the thermal hydrolytic stability of ILs is a key parameter that determines their possible future applications, we studied the stability of $[C_1C_2Im][EtSO_4]$ in the presence of 2–20 mol equiv of water at 353 K, as reported in Table 6. Hydrolysis experiments were performed with 0.01 mol of IL and 0.02–0.20 mol of water in Teflon-lined autoclaves (20 mL capacity). A comparison of the density of the IL–H₂O mixtures measured in each case at 298.15 K and 0.1 MPa before (ρ_i) and after treatment (ρ_m) showed no significant change, even after keeping the mixture at 353 K for 48 h. The observed hydrolytic stability was also confirmed by ¹H NMR. This behavior was surprising given that previous reports had highlighted extremely rapid hydrolysis of the same IL, albeit, in 100 mol equiv of water at 368 K.²⁰

As reactions conducted at 353 K showed no evidence of degradation, increases in reaction temperature, water content, and time were investigated, the details of which are highlighted in Table 7. In general, increases in temperature, water content, and reaction times resulted in higher degrees of degradation for

Table 6. Density Data of $[\text{C}_1\text{C}_2\text{Im}][\text{EtSO}_4] + \text{H}_2\text{O}$ Mixtures Measured at 298.15 K and 0.1 MPa before (ρ_i) and after (ρ_m) Treatment^a

entry	mole ratio IL:H ₂ O	t/h	$\rho_i/\text{g}\cdot\text{cm}^{-3}$	$\rho_m/\text{g}\cdot\text{cm}^{-3}$
1	1:2	1	1.2020	1.2024
2	1:5	1	1.1670	1.1660
3	1:5	3	1.1670	1.1664
4	1:5	24	1.1670	1.1669
5	1:5	48	1.1670	1.1674
6	1:10	1	1.1237	1.1235
7	1:20	1	1.0809	1.0807

^aFor example, $[\text{C}_1\text{C}_2\text{Im}][\text{EtSO}_4]$ heated at 353 K with various molar equivalents of water. Reactions were conducted in a sealed autoclave with headspace.

Table 7. Thermal Hydrolytic Conversion of $[\text{C}_1\text{C}_2\text{Im}][\text{EtSO}_4]$ to $[\text{C}_1\text{C}_2\text{Im}][\text{HSO}_4]$ at a Range of Temperatures with Varying Mole Ratios of Water^a

entry	T/K	mole ratio IL:H ₂ O	t/h	% conv ^b
1	383	1:2	18	0
2	383	1:5	18	0
3	403	1:2	18	5
4	403	1:5	18	16
5	423	1:2	18	13
6	423	1:5	18	31
7	423	1:1	72	0
8	423	1:2	72	72
9	423	1:5	72	87
10	423	1:10	72	87
11 ^c	423 ^c	1:10 ^c	18 ^c	>98 ^c

^aReactions were conducted in sealed autoclave with headspace. ^bConversion measured by ¹H NMR. ^cReaction conducted in an open vessel.

$[\text{C}_1\text{C}_2\text{Im}][\text{EtSO}_4]$, as observed by ¹H NMR and exemplified, herein, in Figure S7 of the Supporting Information. For example, an increase in temperature from 383 to 403 to 423 K with double the molar amount of water present resulted in small increases in degradation from 0% to 5% to 13%, respectively (see Table 7 entries 1, 3, and 5). Although these conversions appear to be low, even small amounts of degradation can significantly impact thermophysical properties.¹⁹ Similar trends in degradation were also observed for analogous reactions conducted using 5 mol equiv of water (see Table 7 entries 2, 4, and 6). Significant increases in degradation were observed by ¹H NMR (see Figure 2) for reactions conducted at 423 K, with up to 87% degradation observed after 72 h in the presence of 5 or 10 mol equiv of water, as reported in Table 7 (entries 9 and 10). Interestingly, for reactions conducted in sealed vessels with a headspace, the volume of water added was critical for high conversions. For example, in an equimolar mixture of IL and H₂O, no conversion was observed at 423 K, probably due to the majority of the water being in the headspace and, therefore, unable to react, as reported in Table 7 (entry 7). Moreover, the small increases in conversion from 72% to 87% on increasing the water content from 2 to 5 to 10 mol (Table 7, entries 8–10) suggests that an equilibrium is present between the headspace phase and the reactant liquid phase.

In this regard, when the thermal hydrolysis of $[\text{C}_1\text{C}_2\text{Im}][\text{EtSO}_4]$ was conducted in an open vessel, almost complete conversion was observed due to the removal of ethanol, as

reported in Table 7, entry 11. When this IL was dried under vacuum overnight at 333 K, as reported in Figure S8 of the Supporting Information, a large difference of viscosity is first observed between pure $[\text{C}_1\text{C}_2\text{Im}][\text{EtSO}_4]$ sample and that measured after vacuum treatment. Furthermore, ¹H NMR and density measurements at 298.15 K ($\rho = 1.3647 \text{ g}\cdot\text{cm}^{-3}$) were almost identical to those reported for $[\text{C}_1\text{C}_2\text{Im}][\text{HSO}_4]$ in the literature,^{24,31} as well as that of an authentic sample of the same IL purchased from BASF measured in our laboratory (see Table 2). Further evidence for a thermodynamic equilibrium was observed when a similar reaction conducted in a sealed vessel with no headspace resulted in 27% conversion to the equivalent $[\text{HSO}_4]^-$ -based IL after 4 h. Thereafter, no further change was observed upon heating for a further 24 h.⁴⁴

A range of other ILs was also tested for thermal hydrolytic stability at 423 K with 5 mol equiv of water, as reported in Table 8. All reactions were conducted in Teflon-sealed reactors. For the methyl sulfate-based ILs (Table 8, entries 1–4) significant conversions were observed, which were independent of the choice of cation (see Figures S9–S12 in the Supporting Information). Unsurprisingly, and as reported in Table 8 (entries 5–7), increasing the alkyl chain length of the sulfate anion resulted in an increase in thermohydrolytic stability. Despite the increase in stability, the octyl sulfate anion showed up to 32% degradation under the experimental conditions after 2 months (Table 8, entry 8), as shown in Figure S13 of the Supporting Information. This unexpected result is in fact in contradiction with all conclusions reported into the literature regarding the hydrolytic stability of this anion.¹⁶

Transesterification Reaction of Hydrogen Sulfate-Based ILs with Alcohols. On the basis of the knowledge that alkyl sulfate ILs show different hydrolytic stabilities, we focused our study on the stability of $[\text{C}_1\text{C}_2\text{Im}][\text{HSO}_4]$ IL in the presence of methanol and ethanol. Experiments were again conducted in a sealed vessel without a headspace using 2.5 mol equiv of each alcohol at 423 K, the results of which are detailed in Table 9. From the table, it can be concluded that the $[\text{HSO}_4]^-$ IL is not stable in the presence of either methanol and ethanol (see Figures S14–S16 of the Supporting Information). This result is in fact in good agreement with the thermodynamic equilibrium observed during the investigation of the thermal hydrolytic stability of $[\text{C}_1\text{C}_2\text{Im}][\text{EtSO}_4]$.

The thermal stability of the $[\text{C}_1\text{C}_2\text{Im}][\text{HSO}_4]$ was also examined in the presence of other alcohols with longer chain lengths such as 1-butanol or 1-octanol. Unexpectedly, we observed that the $[\text{C}_1\text{C}_2\text{Im}][\text{HSO}_4] + 1$ -butanol and $[\text{C}_1\text{C}_2\text{Im}][\text{HSO}_4] + 1$ -octanol binary mixtures are only partially miscible at room temperature. From ¹H NMR measurements,³⁴ at 293.15 K the 1-butanol mole fraction in the $[\text{C}_1\text{C}_2\text{Im}][\text{HSO}_4]$ -rich phase is $x_{1\text{-butanol}} = 0.375$, while the $[\text{C}_1\text{C}_2\text{Im}][\text{HSO}_4]$ mole fraction is close to 0.048 in the 1-butanol-rich phase. Similarly, at 293.15 K the 1-octanol mole fraction in the $[\text{C}_1\text{C}_2\text{Im}][\text{HSO}_4]$ -rich phase is $x_{1\text{-octanol}} = 0.004$, while the $[\text{C}_1\text{C}_2\text{Im}][\text{HSO}_4]$ mole fraction is close to 0.005 in the 1-octanol-rich phase. In other words, the immiscibility region of $[\text{C}_1\text{C}_2\text{Im}][\text{HSO}_4] + n$ -alcohol increases with the alkyl chain length, which can be linked to the increase of the van der Waals force in the solution. Such information can also be associated with the increase of thermal hydrolytic stability observed with the increase of the alkyl chain length on the alkyl sulfate anion. To investigate the stability of the $[\text{C}_1\text{C}_2\text{Im}][\text{HSO}_4]$ IL with 1-butanol and 1-octanol, the liquid + liquid miscibility gap was measured in both cases using a standard nephelometric method.^{22,33} Clear and cloud point temperatures

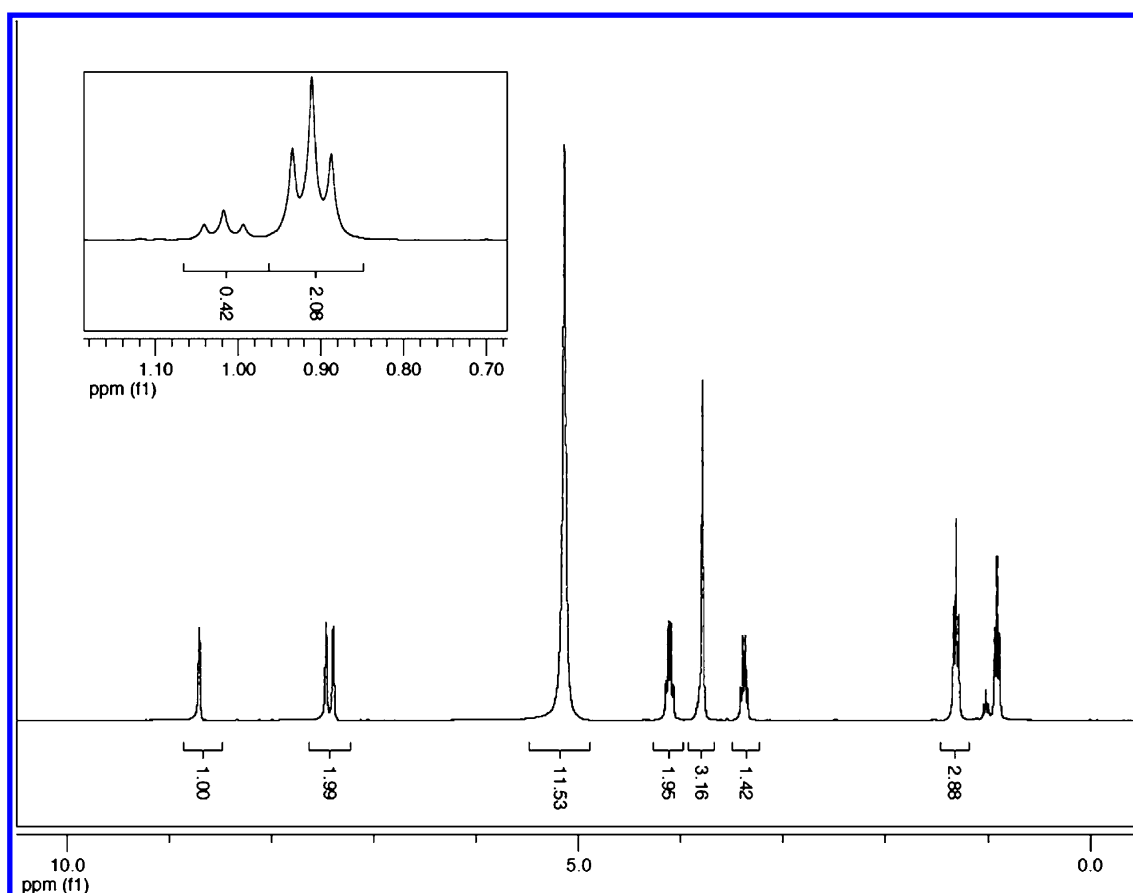


Figure 2. ^1H NMR spectrum showing the hydrolysis reaction between $[\text{C}_1\text{C}_2\text{Im}][\text{EtSO}_4]$ and 10 mol equiv of water at 423 K, forming ethanol and $[\text{C}_1\text{C}_2\text{Im}][\text{HSO}_4]$.

Table 8. Thermal Hydrolytic Conversion of Various Alkyl Sulfate-Based ILs after Treating the Mixture Containing 1:5 Mol Ratios of IL:H₂O at 423 K over 18 h (entry 8, after 2 months)^a

entry	cation	anion	% conv ^b
1	$[\text{C}_1\text{C}_2\text{Im}]^+$	$[\text{MeSO}_4]^-$	53
2	$[\text{C}_1\text{C}_4\text{Im}]^+$		51
3	$[\text{C}_1\text{C}_4\text{Pyrro}]^+$		49
4	$[\text{N}_{1444}]^+$		26
5	$[\text{C}_1\text{C}_2\text{Im}]^+$	$[\text{MeSO}_4]^-$	51
6		$[\text{EtSO}_4]^-$	28
7		$[\text{OctSO}_4]^-$	<2
8 ^c		$[\text{OctSO}_4]^-$	32 ^c

^aReactions were conducted in sealed autoclave with headspace.

^bConversion measured by ^1H NMR. ^cAfter 2 months.

Table 9. Reaction of $[\text{C}_1\text{C}_2\text{Im}][\text{HSO}_4]$ with 2.5 Mol Equiv of Alcohol at 423 K over 18 h^a

entry	ROH	% conv ^b
1	MeOH	51
2	EtOH	51

^aReaction were conducted in sealed autoclave without headspace.

^bConversion measured by ^1H NMR.

were systematically investigated as reported in the Figure 3. In the case of the $[\text{C}_1\text{C}_2\text{Im}][\text{HSO}_4]$ + 1-butanol binary mixture, during the first heating cycle, the upper critical solution temperature (UCST) is observed at $x_{1\text{-butanol}} = 0.6$ and 317.15

K. Similarly, the UCST was reached at $x_{1\text{-octanol}} = 0.5$ and 443.15 K in the case of the $[\text{C}_1\text{C}_2\text{Im}][\text{HSO}_4]$ + 1-octanol mixture. Surprisingly, in both cases large differences are observed between clear and cloud point temperatures (up to 82 K) in the case of the $[\text{C}_1\text{C}_2\text{Im}][\text{HSO}_4]$ + 1-octanol binary mixture. In the case of $[\text{C}_1\text{C}_2\text{Im}][\text{HSO}_4]$ + 1-butanol, no cloud point is then observed by decreasing the temperature down to room temperature (293.15 K) for each individual composition studied during this work (still a one-phase system). In the case of $[\text{C}_1\text{C}_2\text{Im}][\text{HSO}_4]$ + 1-octanol, no cloud point is then observed after maintaining the temperature at 433.15 K for 5 h for each individual composition investigated herein. In other words, rapid transesterification is observed between $[\text{C}_1\text{C}_2\text{Im}][\text{HSO}_4]$ and 1-butanol and between $[\text{C}_1\text{C}_2\text{Im}][\text{HSO}_4]$ and 1-octanol. In both cases, ^1H NMR and ^{13}C NMR spectra confirm the transesterification reaction between the hydrogen sulfate and the alcohol (see Figures S17 and 18 of the Supporting Information, respectively). After reaction, the product from the equimolar mixtures of $[\text{C}_1\text{C}_2\text{Im}][\text{HSO}_4]$ with 1-butanol or of $[\text{C}_1\text{C}_2\text{Im}][\text{HSO}_4]$ with 1-octanol was dried under vacuum overnight at 433 K. The density of each product was then measured at 298.15 K and 0.1 MPa, giving values of 1.1760 and 1.0895 $\text{g}\cdot\text{cm}^{-3}$ in the case of the $[\text{C}_1\text{C}_2\text{Im}][\text{HSO}_4]$ + 1-butanol and $[\text{C}_1\text{C}_2\text{Im}][\text{HSO}_4]$ + 1-octanol binary mixtures, respectively. In other words, each product has NMR spectra and density at 298.15 K close to those observed in the case of $[\text{C}_1\text{C}_2\text{Im}][\text{BuSO}_4]$ ²⁴ and of $[\text{C}_1\text{C}_2\text{Im}][\text{OcSO}_4]$,^{24,29} respectively. In both cases, rapid transesterification is observed. These results mirror those obtained in the hydrolysis experiments, that the octyl sulfate-based IL is more

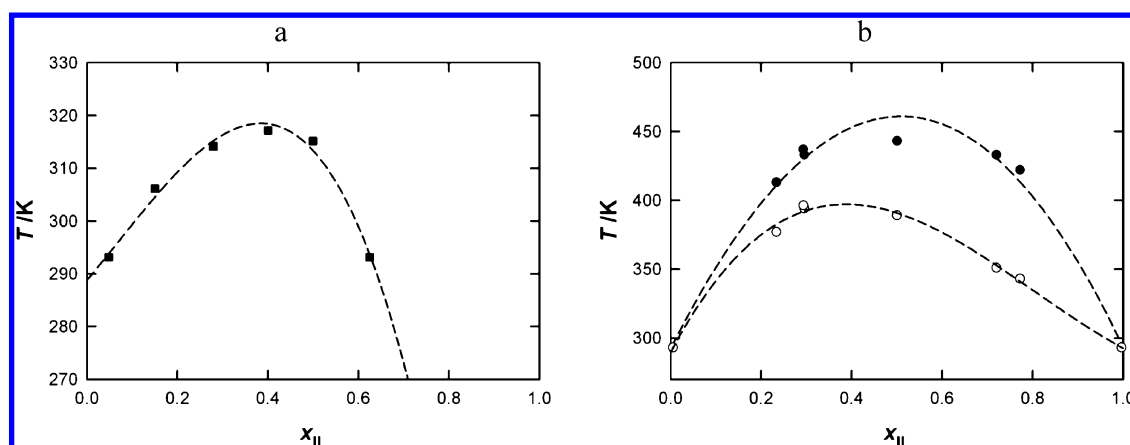


Figure 3. “LLE coexistence curves” demonstrating the transesterification reaction between (a) $[\text{C}_1\text{C}_2\text{Im}][\text{HSO}_4] + 1\text{-butanol}$, where each \blacksquare represents the first observed clear point at a composition expressed in IL mole fraction x_{IL} (no cloud point is then observed after cooling the temperature down to 293 K); (b) $[\text{C}_1\text{C}_2\text{Im}][\text{HSO}_4] + 1\text{-octanol}$, where each \bullet or \circ represents the first observed clear and cloud points at a composition expressed in IL mole fraction x_{IL} , respectively. Each dashed line is for guidance only.

Table 10. Estimated Thermochemistry Properties Using G3 Calculations for Each Individual Compound Involved during This Work as a Function of Temperature from 298.15 to 423.15 K

compd	G3(0K)	G3 energy	G3 enthalpy	G3 free energy	ZPE
$T = 298.15 \text{ K}$					
water	-76.38204	-76.37920	-76.37826	-76.39963	0.02052
$[\text{HSO}_4]^-$	-699.50093	-699.49600	-699.49505	-699.52954	0.02655
methanol	-115.62922	-115.62587	-115.62492	-115.65195	0.04940
ethanol	-154.90475	-154.90039	-154.89944	-154.93017	0.07680
1-butanol	-233.44605	-233.43904	-233.43810	-233.47632	0.13142
1-octanol	-390.53036	-390.51778	-390.51683	-390.56994	0.24035
$[\text{MeSO}_4]^-$	-738.75680	-738.75064	-738.74970	-738.78727	0.05408
$[\text{EtSO}_4]^-$	-778.03307	-778.02557	-778.02462	-778.06624	0.08112
$[\text{BuSO}_4]^-$	-856.57538	-856.56505	-856.56411	-856.61341	0.13553
$[\text{OcSO}_4]^-$	-1013.66658	-1013.65069	-1013.64974	-1013.71066	0.24414
$T = 383.15 \text{ K}$					
water	-76.38204	-76.37838	-76.37717	-76.40587	0.02052
$[\text{HSO}_4]^-$	-699.50096	-699.49368	-699.49246	-699.53986	0.02653
methanol	-115.62922	-115.62455	-115.62334	-115.65985	0.04940
ethanol	-154.90475	-154.89830	-154.89709	-154.93921	0.07681
1-butanol	-233.44605	-233.43541	-233.43420	-233.48770	0.13142
1-octanol	-390.53036	-390.51105	-390.50984	-390.58596	0.24035
$[\text{MeSO}_4]^-$	-738.75680	-738.74763	-738.74641	-738.79843	0.05408
$[\text{EtSO}_4]^-$	-778.03308	-778.02176	-778.02055	-778.07870	0.08112
$[\text{BuSO}_4]^-$	-856.57538	-856.55970	-856.55849	-856.62817	0.13553
$[\text{OcSO}_4]^-$	-1013.66658	-1013.64222	-1013.64101	-1013.73022	0.24414
$T = 423.15 \text{ K}$					
water	-76.38204	-76.37799	-76.37665	-76.40890	0.02052
$[\text{HSO}_4]^-$	-699.50096	-699.49247	-699.49113	-699.54487	0.02653
methanol	-115.62922	-115.62386	-115.62252	-115.66370	0.04940
ethanol	-154.90475	-154.89717	-154.89583	-154.94368	0.07681
1-butanol	-233.44605	-233.43343	-233.43209	-233.49339	0.13142
1-octanol	-390.53036	-390.50735	-390.50601	-390.59410	0.24035
$[\text{MeSO}_4]^-$	-738.75680	-738.74604	-738.74470	-738.80395	0.05408
$[\text{EtSO}_4]^-$	-778.03308	-778.01974	-778.01840	-778.08488	0.08112
$[\text{BuSO}_4]^-$	-856.57538	-856.55682	-856.55548	-856.63559	0.13553
$[\text{OcSO}_4]^-$	-1013.66658	-1013.63761	-1013.63627	-1013.74000	0.24414

hydrolytically stable than the corresponding methyl or ethyl sulfate-based ILs. In other words, hydrogen sulfate-based ILs are unstable in presence of alcohols, which can be seen as an advantage for the separation of alcohol in a liquid mixture as well as the starting point for the formation of new family of alkyl

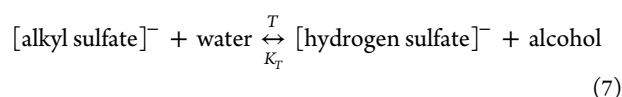
sulfate anions. For example, perfluoro alcohol (2,2,3,3,4,4,4-heptafluoro-1-butanol) and an aromatic ring alcohol (benzyl alcohol) both reacted at 383 K to form the corresponding alkyl and aryl sulfate anion (see Figures S19–S20 of the Supporting Information). An amino alcohol (*N,N*-diisopropylaminoetha-

Table 11. Hydrolysis Equilibrium Constants (K_T) and Transesterification Equilibrium Constants (K_T^{-1}) Calculated by Using Eqs 7–10 with Values Reported in Table 10 as a Function of Temperature from 298.15 to 423.15 K

anion	T = 298.15 K		T = 383.15 K		T = 423.15 K	
	K_T	K_T^{-1}	K_T	K_T^{-1}	K_T	K_T^{-1}
[MeSO ₄] [−]	0.00323	309.73	0.0226	44.20	0.0411	24.33
[EtSO ₄] [−]	0.00147	681.43	0.0107	93.61	0.0201	49.63
[BuSO ₄] [−]	0.000496	2015.0	0.00477	209.7	0.00959	104.3
[OcSO ₄] [−]	0.0000105	94862	0.000208	4801	0.000603	1658

anol) was also reacted with [C₁C₂Im][HSO₄], rapidly forming a highly viscous material at 293K (see Figure S21 in the Supporting Information). A similar rapid reaction was also observed when [C₁C₂Im][HSO₄] was reacted with butylamine, forming a solid material. In both of these cases, the exact structure of the new IL is currently under investigation (see Figure S22 in the Supporting Information).

Thermodynamic Equilibrium between Hydrolysis and Transesterification Reactions. The standard procedure for estimating thermochemistry values from Gaussian has been used,⁴⁵ by using the optimized ideal gas phase structure of all species as a function of temperature. Herein this was performed using HF within Gaussian version 3.0,⁴⁶ by means of using the 6-31G(d) basis set. The resultant optimized structure for each molecule is subsequently then used to calculate the thermochemistry values using the G3 method,⁴⁵ from which different outputs like the G3(0K), the total electronic energy as defined by the compound model, including the zero-point energy (ZPE) scaled by the factor defined in the model ($\epsilon_0 + \epsilon_{ZPE}$); the G3 energy, the total electronic energy plus the internal thermal energy, which already includes the ZPE ($\epsilon_0 + E_{tot}$); the G3 enthalpy, the sum of the total electronic energy and thermal enthalpies ($\epsilon_0 + H_{corr}$); and the G3 free energy, the sum of the total electronic energy and thermal free energies ($\epsilon_0 + G_{corr}$), are obtained for each specie involved in the following hydrolysis/transesterification reaction



where [alkyl sulfate][−] is the methyl, ethyl, butyl, or octyl sulfate anion, the alcohol structure is then obtained from the corresponding [alkyl sulfate][−] anion, T is the studied temperature set as equal to 298.15, 383.15, and 423.15 K, and K_T is the equilibrium constant in the case of the hydrolysis reaction, calculated according to the following equations

$$\Delta_r H^\circ(T) = \sum (\epsilon_0 + H_{corr})_{\text{products}} - \sum (\epsilon_0 + H_{corr})_{\text{reactants}} \quad (8)$$

$$\Delta_r G^\circ(T) = \sum (\epsilon_0 + G_{corr})_{\text{products}} - \sum (\epsilon_0 + G_{corr})_{\text{reactants}} \quad (9)$$

$$K_T = \exp\left(-\frac{\Delta_r G^\circ(T)}{RT}\right) \quad (10)$$

where $\Delta_r H^\circ(T)$ is the enthalpy of reaction and $\Delta_r G^\circ(T)$ is the enthalpy of reaction calculated at the temperature T , R is the universal gas constant ($R = 1.9859 \text{ cal}\cdot\text{mol}^{-1}\cdot\text{K}^{-1}$), and K_T is the hydrolysis equilibrium constant, from which the transesterification equilibrium constant can be calculated as equal to K_T^{-1} .

By using this methodology, the energy of each individual species was investigated during this work and reported at 298.15, 383.15 and 423.15 K in Table 10. By using data from this table

and eqs 7–10, hydrolysis equilibrium constants (K_T) and transesterification equilibrium constants (K_T^{-1}) were then deduced for all reactions between water and an [alkyl sulfate][−] (methyl, ethyl, butyl, or octyl sulfate) anion and are reported, herein, in Table 11. From the Tables 10 and 11, and as expected from the experimental results, it appears that each investigated reaction is driven by a thermodynamic equilibrium. Furthermore, it can be observed that the hydrolysis reaction described in eq 7 increases by increasing the temperature. In the case of the ethyl sulfate hydrolysis reaction, K_T increases up to 20 times by increasing the temperature from 298.15 to 423.15 K; a similar observation is made for each alkyl sulfate investigated during this work, as shown in Table 11. On the basis of results reported in Tables 10 and 11, it appears also that the hydrolysis reaction is more favorable in the case of the anion having a short chain length such as the methyl and ethyl sulfate, where K_T values are close to 0.04 and 0.02 at 423 K, respectively. In the case of the hydrolysis reaction involving the ethyl sulfate-based ILs, the calculated K_T value is in agreement (same order of magnitude) with that observed experimentally (experimental $K_T \approx 0.07$) by using a sealed vessel without a headspace.⁴⁴ It appears, finally, that the hydrolysis thermodynamic equilibrium constant decreases, as expected from experimental value, with the alkyl chain length on the alkyl sulfate anion, a contrario of the transesterification equilibrium constants K_T^{-1} . For alkyl sulfate anions containing a long chain length, such as found in butyl or octyl sulfate, K_T values are 1 or 2 orders of magnitude lower than those observed in the case of methyl and ethyl sulfate, which can explain why hydrolysis products are obtained after a few months of reaction in the case of the octyl sulfate anion. Additionally, and as observed experimentally, a favorable transesterification reaction is predicted during these calculations by mixing 1-octanol (or 1-butanol) with [HSO₄][−] anion, as its equilibrium constants K_T^{-1} is close to 1658 (or 104) at 423 K.

CONCLUSION

During this work the volumetric properties of a series of alkyl sulfate ILs as a function of temperature are reported. From this study we extended our group contribution models to explain some anomalies in density measurements compared with those reported previously in the literature. This was explained by the hydrolytic instability of aprotic alkyl sulfate anion-based ILs and prompted us to further investigate their hydrolytic stability. Therein, the role of the cation, i.e., imidazolium, ammonium, or pyrrolidinium, played a minimal role in the IL stability with water. However, the anion played a crucial role in determining the rate of hydrolysis of the IL, with longer chain alkyl sulfate anion systems such as 1-octyl and 1-butyl showing increased stability compared to methyl and ethyl sulfate-based ILs. Despite the increased stability of the octyl sulfate system, degradation to the corresponding 1-octanol and hydrogen sulfate IL was observed, albeit, after a few months at 423 K. This instability

could help to explain the biodegradability of this alkyl sulfate IL family.

The observed hydrolytic instability is thermodynamically driven, and therefore, competition between hydrolysis and transesterification is observed. The balance between the two reactions depends on the alkyl sulfate chain length, affinity, and mutual solubility of the component mixtures. For example, mixtures of $[C_1C_2Im][HSO_4]$ and alcohols react to form the corresponding alkyl sulfate and water, with rapid synthesis of butyl and octyl sulfate ILs being observed when the mixture is heated above the UCST. The partial miscibility of hydrogen sulfate and 1-octanol can help to explain the increased stability of oyl sulfate ionic liquids. This type of reaction has the potential to be employed for separation of alcohols as well as forming novel alkyl sulfate-based ionic liquids using aromatic alcohols, perfluoro alcohols, amino alcohols, and amines without the use of a catalyst.

■ ASSOCIATED CONTENT

● Supporting Information

1H and ^{13}C NMR spectra recorded during this work are provided in Figures S1–S6 and S7–S23 in the case of pure ILs and of their reactions with water or alcohol, respectively. This material is available free of charge via the Internet at <http://pubs.acs.org>

■ AUTHOR INFORMATION

Corresponding Author

*E-mail: johan.jacquemin@qub.ac.uk (J.J.); p.goodrich@qub.ac.uk (P.G.).

Notes

The authors declare no competing financial interest.

■ ACKNOWLEDGMENTS

The authors would like to thank Dr. Alfonso Pensado from Wilhelm-Ostwald Institute of Physical and Theoretical Chemistry of the University of Leipzig for his useful suggestions regarding Gaussian calculations.

■ REFERENCES

- (1) Esperanca, J.; Lopes, J. N. C.; Tariq, M.; Santos, L.; Magee, J. W.; Rebelo, L. P. N. Volatility of aprotic ionic liquids—A review. *J. Chem. Eng. Data* **2010**, *55*, 3–12.
- (2) Earle, M. J.; Esperanca, J.; Gilea, M. A.; Lopes, J. N. C.; Rebelo, L. P. N.; Magee, J. W.; Seddon, K. R.; Widegren, J. A. The distillation and volatility of ionic liquids. *Nature* **2006**, *439*, 831–834.
- (3) Siedlecka, E. M.; Czerwicka, M.; Stolte, S.; Stepnowski, P. Stability of ionic liquids in application conditions. *Curr. Org. Chem.* **2011**, *15*, 1974–1991.
- (4) Jacquemin, J.; Husson, P.; Padua, A. A. H.; Majer, V. Density and viscosity of several pure and water-saturated ionic liquids. *Green Chem.* **2006**, *8*, 172–180.
- (5) Jacquemin, J.; Ge, R.; Nancarrow, P.; Rooney, D. W.; Costa Gomes, M. F.; Padua, A. A. H.; Hardacre, C. Prediction of ionic liquid properties. I. Volumetric properties as a function of temperature at 0.1 MPa. *J. Chem. Eng. Data* **2008**, *53*, 716–726.
- (6) Husson, P.; Pison, L.; Jacquemin, J.; Gomes, M. F. C. Influence of water on the carbon dioxide absorption by 1-ethyl-3-methylimidazolium bis(trifluoromethylsulfonyl)amide. *Fluid Phase Equilib.* **2010**, *294*, 98–104.
- (7) Seddon, K. R.; Stark, A.; Torres, M. J. Influence of chloride, water, and organic solvents on the physical properties of ionic liquids. *Pure Appl. Chem.* **2000**, *72*, 2275–2287.
- (8) Troncoso, J.; Cerdeirina, C. A.; Sanmamed, Y. A.; Romani, L.; Rebelo, L. P. N. Thermodynamic properties of imidazolium-based ionic liquids: Densities, heat capacities, and enthalpies of fusion of

$[bmim][PF_6]$ and $[bmim][NTf_2]$. *J. Chem. Eng. Data* **2006**, *51*, 1856–1859.

(9) Carvalho, P. J.; Regueira, T.; Santos, L.M.N.B.F.; Fernandez, J.; Coutinho, J. A. P. Effect of water on the viscosities and densities of 1-butyl-3-methylimidazolium dicyanamide and 1-butyl-3-methylimidazolium tricyanomethane at atmospheric pressure. *J. Chem. Eng. Data* **2010**, *55*, 645–652.

(10) Spohr, H. V.; Patey, G. N. The influence of water on the structural and transport properties of model ionic liquids. *J. Chem. Phys.* **2010**, *132*, 234510–1–13.

(11) Goodrich, B. F.; De La Fuente, J. C.; Gurkan, B. E.; Lopez, Z. K.; Price, E. A.; Huang, Y.; Brennecke, J. F. Effect of water and temperature on absorption of CO_2 by amine-functionalized anion-tethered ionic liquids. *J. Phys. Chem. B* **2011**, *115*, 9140–9150.

(12) Swatloski, R. P.; Holbrey, J. D.; Rogers, R. D. Ionic liquids are not always green: Hydrolysis of 1-butyl-3-methylimidazolium hexafluorophosphate. *Green Chem.* **2003**, *5*, 361–363.

(13) Freire, M. G.; Neves, C. M. S. S.; Marrucho, I. M.; Coutinho, J. A. P.; Fernandes, A. M. Hydrolysis of tetrafluoroborate and hexafluorophosphate counter ions in imidazolium-based ionic liquids. *J. Phys. Chem. A* **2010**, *114*, 3744–3749.

(14) Părvulescu, V. I.; Hardacre, C. Catalysis in ionic liquids. *Chem. Rev.* **2007**, *107*, 2615–2665.

(15) Eßer, J.; Wasserscheid, P.; Jess, A. Deep desulfurization of oil refinery streams by extraction with ionic liquids. *Green Chem.* **2004**, *6*, 316–322.

(16) Wasserscheid, P.; Van Hal, R.; Bösmann, A. 1-*n*-Butyl-3-methylimidazolium ($[bmim]$) octylsulfate—An even ‘greener’ ionic liquid. *Green Chem.* **2002**, *4*, 400–404.

(17) Ficke, L. E.; Rodriguez, H.; Brennecke, J. F. Heat capacities and excess enthalpies of 1-ethyl-3-methylimidazolium-based ionic liquids and water. *J. Chem. Eng. Data* **2008**, *53*, 2112–2119.

(18) Jacquemin, J.; Husson, P.; Majer, V.; Cibulka, I. High-pressure volumetric properties of imidazolium-based ionic liquids: Effect of the anion. *J. Chem. Eng. Data* **2007**, *52*, 2204–2211.

(19) Jacquemin, J.; Husson, P. Comments and additional work on “High-pressure volumetric properties of imidazolium-based ionic liquids—Effect of the anion” [*J. Chem. Eng. Data* **2007**, *52*, 2204–2211]. *J. Chem. Eng. Data* **2012**, *57*, 2409–2414.

(20) Himmler, S.; Hörmann, S.; van Hal, R.; Schulz, P.; Wasserscheid, P. Transesterification of methylsulfate and ethylsulfate ionic liquids—An environmentally benign way to synthesize long-chain and functionalized alkylsulfate ionic liquids. *Green Chem.* **2006**, *8*, 887–894.

(21) Ferguson, J. L.; Holbrey, J. D.; Ng, S.; Plechkova, N. V.; Seddon, K. R.; Tomaszowska, A. A.; Wassell, D. F. A greener, halide-free approach to ionic liquid synthesis. *Pure Appl. Chem.* **2012**, *84*, 723–744.

(22) Wang, S.; Jacquemin, J.; Husson, P.; Hardacre, C.; Costa Gomes, M. F. Liquid–liquid miscibility and volumetric properties of aqueous solutions of ionic liquids as a function of temperature. *J. Chem. Thermodyn.* **2009**, *41*, 1206–1214.

(23) Pereiro, A. B.; Verdía, P.; Tojo, E.; Rodriguez, A. Physical Properties of 1-butyl-3-methylimidazolium methyl sulfate as a function of temperature. *J. Chem. Eng. Data* **2007**, *52*, 377–380.

(24) Costa, A. J. L.; Esperança, J. M. S. S.; Marrucho, I. M.; Rebelo, L. P. N. Densities and viscosities of 1-ethyl-3-methylimidazolium *n*-alkyl sulfates. *J. Chem. Eng. Data* **2011**, *56*, 3433–3441.

(25) Gonzalez, B.; Gomez, E.; Dominguez, A.; Vilas, M.; Tojo, E. Physicochemical characterization of new sulfate ionic liquids. *J. Chem. Eng. Data* **2011**, *56*, 14–20.

(26) Gomez, E.; Gonzalez, B.; Calvar, N.; Tojo, E.; Dominguez, A. Physical properties of pure 1-ethyl-3-methylimidazolium ethylsulfate and its binary mixtures with ethanol and water at several temperatures. *J. Chem. Eng. Data* **2006**, *51*, 2096–2102.

(27) Kumelan, J.; Perez-Salado Kamps, A.; Tuma, D.; Maurer, G. Solubility of CO_2 in the Ionic Liquids $[bmim][CH_3SO_4]$ and $[bmim][PF_6]$. *J. Chem. Eng. Data* **2006**, *51*, 1802–1807.

(28) Navia, P.; Troncoso, J.; Romani, L. Excess magnitudes for ionic liquid binary mixtures with a common ion. *J. Chem. Eng. Data* **2007**, *52*, 1369–1374.

- (29) Russina, O.; Gontrani, L.; Fazio, B.; Lombardo, D.; Triolo, A.; Caminiti, R. Selected chemical-physical properties and structural heterogeneities in 1-ethyl-3-methylimidazolium alkyl-sulfate room temperature ionic liquids. *Chem. Phys. Lett.* **2010**, *493*, 259–262.
- (30) de Castro, C. A. N.; Langa, E.; Morais, A. L.; Lopes, M. L. M.; Lourenço, M. J.; Santos, F. J.; Santos, M. S. C.; Lopes, J. N. C.; Veiga, H. I.; Macatrão, M.; Esperança, J. M. S. S.; Marques, C. S.; Rebelo, L. P.; Afonso, C. A. Studies on the density, heat capacity, surface tension and infinite dilution diffusion with the ionic liquids [C₄mim][NTf₂], [C₄mim][dca], [C₂mim][EtOSO₃] and [Aliquat][dca]. *Fluid Phase Equilib.* **2010**, *294*, 157–179.
- (31) Ficke, L. E.; Novak, R. R.; Brennecke, J. F. Thermodynamic and thermophysical properties of ionic liquid + water systems. *J. Chem. Eng. Data* **2010**, *55*, 4946–4950.
- (32) Shekaari, H.; Armanfar, E. Apparent molar volumes and expansivities of aqueous solutions of ionic liquids, 1-alkyl-3-methylimidazolium alkyl sulfate at $T = (298.15–328.15)$ K. *Fluid Phase Equilib.* **2011**, *303*, 120–125.
- (33) Heintz, A.; Lehmann, J. K.; Wertz, C.; Jacquemin, J. Thermodynamic properties of mixtures containing ionic liquids. 4. LLE of binary mixtures of [C₂MIM][NTf₂] with propan-1-ol, butan-1-ol, and pentan-1-ol and [C₄MIM][NTf₂] with cyclohexanol and 1,2-hexanediol including studies of the influence of small amounts of water. *J. Chem. Eng. Data* **2005**, *50*, 956–960.
- (34) Ab Manan, N.; Atkins, M. P.; Jacquemin, J.; Hardacre, C.; Rooney, D. W. Phase equilibria of binary and ternary systems containing ILs, dodecane, and cyclohexanecarboxylic acid. *Sep. Sci. Technol.* **2012**, *47*, 312–324.
- (35) Ramdin, M.; Vlugt, T. J. H.; de Loos, T. W. Solubility of CO₂ in the ionic liquids [TBMN][MeSO₄] and [TBMP][MeSO₄]. *J. Chem. Eng. Data* **2012**, *57*, 2275–2280.
- (36) Davila, M. J.; Aparicio, S.; Alcalde, R.; Garcia, B.; Leal, J. M. On the properties of 1-butyl-3-methylimidazolium octylsulfate ionic liquid. *Green Chem.* **2007**, *9*, 221–232.
- (37) Jacquemin, J.; Husson, P.; Majer, V.; Padua, A. A. H.; Costa Gomes, M. F. Thermophysical properties, low pressure solubilities and thermodynamics of solvation of carbon dioxide and hydrogen in two ionic liquids based on the alkylsulfate anion. *Green Chem.* **2008**, *10*, 944–950.
- (38) Rooney, D. W.; Jacquemin, J.; Gardas, R. Thermophysical properties of ionic liquids. *Top. Curr. Chem.* **2009**, *290*, 185–212.
- (39) Dong, Q.; Muzny, C. D.; Kazakov, A.; Diky, V.; Magee, J. W.; Widegren, J. A.; Chirico, R. D.; Marsh, K. N.; Frenkel, M. ILThermo: A free-access web database for thermodynamic properties of ionic liquids. *J. Chem. Eng. Data* **2007**, *52*, 1151–1159.
- (40) Rebelo, L. P. N.; Najdanovic-Visak, V.; Gomes de Azevedo, R.; Esperança, J. M. S. S.; Nunes da Ponte, M.; Guedes, H. J. R.; de Sousa, H. C.; Szydłowski, J.; Canongia Lopes, J. N.; Cordeiro, T. C. Phase behaviour and thermodynamic properties of ionic liquids, ionic liquid mixtures, and ionic liquid solutions. In *Ionic Liquids IIIA: Fundamentals, Progress, Challenges, and Opportunities—Properties and Structure*; Rogers, R. D., Seddon, K. R., Eds; ACS Symposium Series 901; American Chemical Society: Washington, DC, 2005; Chapter 21, pp 270–291.
- (41) Jacquemin, J.; Nancarrow, P.; Rooney, D. W.; Costa Gomes, M. F.; Pádua, A. A. H.; Hardacre, C. Prediction of ionic liquid properties. II. Volumetric properties as a function of temperature at 0.1 MPa. *J. Chem. Eng. Data* **2008**, *53*, 716–726.
- (42) Anthony, J. L.; Anderson, J. L.; Maginn, E. J.; Brennecke, J. F. Anion effects on gas solubility in ionic liquids. *J. Phys. Chem. B* **2005**, *109*, 6366–6374.
- (43) Domanska, U.; Pobudkowska, A.; Wisniewska, A. Solubility and excess molar properties of 1,3-dimethylimidazolium methylsulfate, or 1-butyl-3-methylimidazolium methylsulfate, or 1-butyl-3-methylimidazolium octylsulfate ionic liquids with *n*-alkanes and alcohols: Analysis in terms of the PFP and FBT models. *J. Solution Chem.* **2006**, *35*, 311–334.
- (44) [C₁C₂Im][EtSO₄]:H₂O molar ratio 1:5, 27% conversion after 4 h, 29% conversion after 8 h, 27% conversion after 18 h, and 27% conversion after 24 h. All conversions were monitored by ¹H NMR.
- (45) http://www.gaussian.com/g_whitepap/thermo.htm viewed online on July 24, 2012.
- (46) Gaussian View 3.0 2000–2003, Gaussian, Inc., Semicem, Inc.; Pittsburgh, PA.